micromachines

MDPI

Article

Dynamic Wet Etching of Silicon through Isopropanol Alcohol Evaporation

Tiago S. Monteiro [1,2], Pamakštys Kastytis [1], Luís M. Gonçalves [2], Graça Minas [2,*] and Susana Cardoso [1,3]

Received: 1 August 2015 ; Accepted: 9 October 2015 ; Published: 15 October 2015
Academic Editor: Joost Lötters

[1] Instituto de Engenharia de Sistemas de Computadores–Microsystems and Nanotechnology (INESC–MN), Rua Alves Redol, Lisboa 1000-029, Portugal; tmonteiro@inesc-mn.pt (T.S.M.); kastytismail@gmail.com (P.K.); scardoso@inesc-mn.pt (S.C.)
[2] Microelectromechanical Systems Research Unit (CMEMS-UMinho), Universidade do Minho, Campus de Azurem, Guimarães 4800-058, Portugal; lgoncalves@dei.uminho.pt
[3] Departamento de Física–Instituto Superior Técnico–Universidade de Lisboa, Av. Rovisco Pais, Lisboa 1000, Portugal
* Correspondence: gminas@dei.uminho.pt; Tel.: +351-253-510190; Fax: +351-253-510189

Abstract: In this paper, Isopropanol (IPA) availability during the anisotropic etching of silicon in Potassium Hydroxide (KOH) solutions was investigated. Squares of 8 to 40 μm were patterned to (100) oriented silicon wafers through DWL (Direct Writing Laser) photolithography. The wet etching process was performed inside an open HDPE (High Density Polyethylene) flask with ultrasonic agitation. IPA volume and evaporation was studied in a dynamic etching process, and subsequent influence on the silicon etching was inspected. For the tested conditions, evaporation rates for water vapor and IPA were determined as approximately 0.0417 mL/min and 0.175 mL/min, respectively. Results demonstrate that IPA availability, and not concentration, plays an important role in the definition of the final structure. Transversal SEM (Scanning Electron Microscopy) analysis demonstrates a correlation between microloading effects (as a consequence of structure spacing) and the angle formed towards the (100) plane.

Keywords: isopropanol evaporation; isopropanol availability; silicon wet etching; microloading effect

1. Introduction

Surface texturing of crystalline silicon wafers is a widely used process in different areas of application. From the solar cell industry [1,2] to MEMS (Microelectromechanical Systems) device fabrication [3–5] and biological applications [6,7], silicon wet etching profile has been studied and improved in order to address the specific requirements that each of these technological fields require.

The silicon wet etching process is a common manufacture process that involves the use of liquid etchants in the removal of exposed areas of the sample. Isotropic or anisotropic profiles can be achieved, depending on the crystalline orientation of the silicon wafer and the etchants used in the process. Regarding anisotropic wet etching, KOH (potassium hydroxide) is the most popular inorganic etchant conventionally used [8]. Although other etchants succeed in achieving a better smoothness, such as the organic compound TMAH (tetramethyl ammonium hydroxide), these are considerably more costly and in most cases neurotoxic, thus presenting a huge health risk that requires the appropriate safety measurements [9–11].

The process at which KOH removes silicon atoms is well described in the literature. Etch rates vary with different crystallographic orientations due to the atomic bonds formed at the surface silicon

atoms. Wafers with a (100) orientation present superficial atoms with two backbonds, connecting to two underlying silicon atoms, and two dangling bonds, capable of suffering a nucleophilic reaction with OH radicals, as shown in Figure 1a. Through the thermal excitation and injection of electrons from the backbond into the conduction band, energy is applied in breaking these bonds and releasing the silicon–hydroxide complex [8].

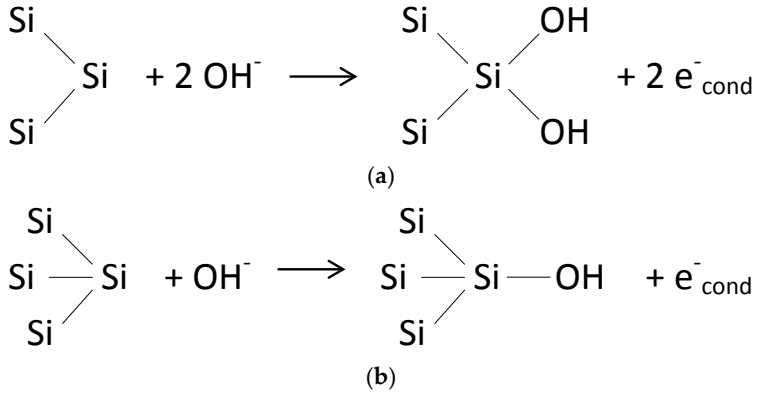

Figure 1. Schematic diagram representing the chemical structure of: surface and respective binding of hydroxide ions during a wet etch process for (**a**) (100) and (**b**) (111) silicon wafers.

Anisotropy is achieved in different crystalline orientations since structural variations are present at the superficial atoms. For a (111) oriented plane, as depicted in Figure 1b, only one dangling bond exists for each superficial atom, thus making it harder to be etched when comparing with a (100) oriented plane, as in Figure 1a [8].

Different chemicals can be used to interact with the surface and compete with OH radicals. Isopropyl Alcohol (IPA) is a widely known molecule that modulates the etching rate of specific crystallographic planes in KOH wet etching processes. Various authors have suggested that IPA acts as a mask, limiting the access of KOH particles to the surface of the Silicon sample [12,13]. However, no chemical reaction seems to be formed between IPA and silicon atoms, thus acting as a mere modulation agent, rather than an etching stop agent [14].

These models for the behavior of IPA molecules at different concentrations take into consideration that, for a saturated concentration, a layer of IPA molecules is formed at the surface of the solution, rather than being diluted. From the proposed models, this abundance of IPA affects the formation of a linear monolayer of alcohol molecules at the surface of the sample [12,13].

Therefore, the final structure at which a silicon wafer is etched is intrinsically dependent on both the crystallographic orientation of the wafer and the type of chemicals used in the etching solution. Precisely controlling the concentration of IPA at any given time is a crucial step in order to achieve a homogeneous etching process.

The silicon wet etching reaction originates byproducts in the form of silicates, $Si(OH)_4$ [8]. If not dispersed from the surface of the sample, these silicates will prevent the continuous etching and act as pseudo-masks, promoting a very rough and heterogeneous etching. Assuring a constant flow between these silicates and fresh OH radicals allows for a better control of the process, improving both smoothness and homogeneity across the entire sample [15].

Conventional KOH wet etch process is usually performed inside a large, closed quartz container with external temperature control. Magnetic stirring of the etching solution allows for a considerable increase in etching homogeneity, creating an internal spiral flow that dilutes the etching byproducts and allows for continuous access to the silicon substrate. However, studies performed by Yang *et al.* [15] have demonstrated that, even with magnetic stirring, defects appear on the surface of the sample as a result of silicates adherence and incomplete hydrogen bubbles detachment.

Ultrasonic agitation plays a great importance in this process, distributing the same amount of vibrational energy throughout the entire solution. This allows for an increase in the efficiency at which particles are interacting with the sample surface and hydrogen bubbles detach [15].

Since both ultrasonic agitation and wet etching are exothermic processes, a minimum working temperature is always established. This temperature varies with the power applied through the agitation and the area of silicon molecules exposed to the etching process. Therefore, samples with considerable larger areas origin higher etching temperatures, and by consequence, higher etching and evaporation rates.

In this study, we present a dynamic wet etching process that allows for a constant control and modulation of two important etching variables: temperature and additives. Through the use of an open container, in which solvent evaporation plays an important role, it is possible to control the impact of specific additives on the etching profile. Therefore, we demonstrate a method combining low temperature (~40 °C) and ultrasounds that provides etching uniformity and control on a low volume experiment (20 mL). It is competitive with conventional high temperature processes. This method has a final impact on the production scale, reducing the energetic and reagents costs.

The experiments have demonstrated that, for the same sample, it is possible to obtain different pyramidal profiles due to microloading effects and additive influence. A wide array of applications is expected for this type of technology in the fields of solar cell industry and MEMS microfabrication. This work was performed to study the etching profile and angles of pyramidal structures to be used in biological cell penetration. Surface topography plays a crucial role, as these structures must be further processed through microfabrication methods.

2. Experimental Details

Experiments were carried out on 0.01–0.03 Ωcm, n-doped, 500 ± 25 μm-thick polished silicon wafers with a monocrystalline (100) orientation (Sil'tronix, Silicon Technologies, Archamps, France). After surface cleaning, with Alconox (Sigma Aldrich 242985 Alconox® detergent, St. Louis, MO, USA) and IPA, a 300 nm thick Chromium layer was deposited by Magnetron Sputtering (Alcatel SCM 450: 3.07 mTorr, 20 sccm Argon, 20 WDC, 51 min [16]). Using Direct Writing Laser photolithography (Lasarray DWL2.0: positive resist PFR 7790 G 1.5 μm-thick [16]), square structures (8 to 40 μm) were defined to study the effect of KOH wet etching and IPA influence over the different crystallographic planes. Profile alignment was performed using the wafers flat and the DWL2.0 software, to a maximum deviation of 0.02 rad. The wafer was then diced in 9 mm × 9 mm individual dies. The resist pattern was transferred to the Cr film by wet etch (Sigma Aldrich 651826 Chromium Etchant, St. Louis, MO, USA). Finally, the Silicon surface is ready to be etched. Notice that any native oxide will be also etched during this process. Because silicon structures to be etched are less than 20 μm thick, the backside of the silicon wafer was left unprotected, with minor impact on the total wafer thickness. The schematic description of the process can be seen in Figure 2.

Twenty-two percent (22 wt %) KOH solutions were prepared by dissolving 70 g of KOH pellets (85% pure, Sigma Aldrich) into approximately 200 mL of distilled water. Since the dissolution of KOH in water is an exothermic process, the solutions were left to cool down overnight before using.

In order to provide a steady and gradual solvent evaporation, low temperatures were aimed for this work. A minimum temperature of 43 °C inside the ultrasonic bath (stabilization temperature achieved after 30 min) was obtained as a consequence of ultrasound agitation. In this work, we demonstrate that even for low temperatures, the quality/uniformity of the etching is competitive with the one obtained with higher temperatures for conventional processes.

Afterwards, the KOH solution was inserted inside a 250 mL HDPE (High Density Polyethylene) flask with a surface area of 28.27 cm^2 and placed inside an ultrasonic bath (Fisher Scientific FB15047, 37 kHz, 30/90 W, Waltham, MA, USA).

A stabilization temperature of about 39 °C, inside the KOH solution, was achieved before the process could continue. At this stage, IPA was added as needed and the sample was placed inside

the wet etching solution. The temperature was measured inside the KOH solution every 5 min using a mercury thermometer. All experiments were conducted inside a clean room at an average temperature of 40 °C ± 1.5 °C.

After the process was completed, the final volume was measured using a graduated HDPE cylinder, for analysis of solvent evaporation.

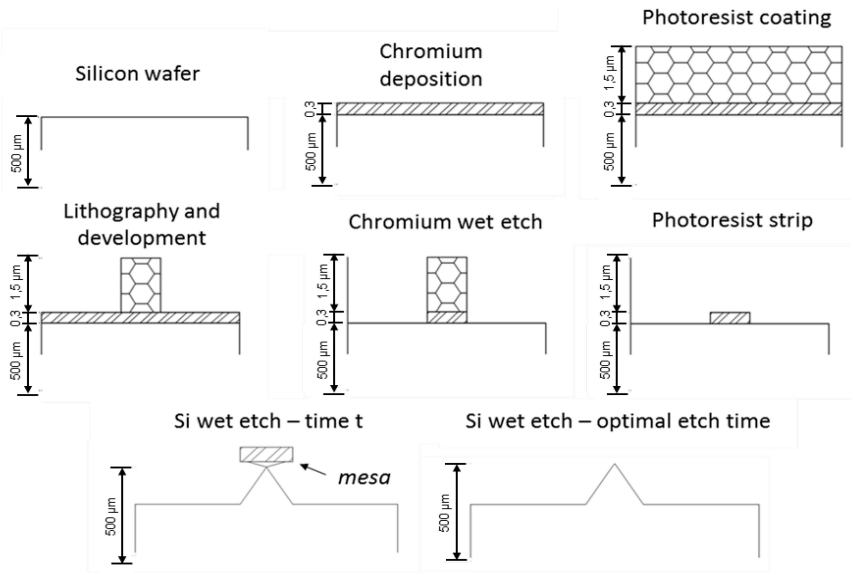

Figure 2. Schematic diagram for the manufacture process of structures through Si wet etch using a Cr mask. A perfect pyramid is obtained after the top mesa mask is released.The instant when this ocurs is defined as optimal etch time.

The samples were then rinsed with distilled water and observed under a microscope to access the progress of the Si etching.

To fully characterize the etching process, the chromium mask layer was removed with chromium etchant, as described before. The samples were then coated with a 5 nm gold layer for SEM (scanning electron microscopy) analysis.

3. Results and Discussion

3.1. Evaporation of Solvents

Since processes run in an open system, the evaporation rate of solvents (IPA and water) should be considered. The final volume of the etching solution was measured and compared to the initial volumes of dissolved KOH and IPA, to evaluate the evaporation rate of water and IPA.

Each experiment started with an initial volume of 20 mL of 22 wt % KOH solution. A control sample, containing no added IPA, and three samples containing 1, 3 and 5 mL of initially added IPA, respectively, Sample B, C and D in Figure 3, underwent a 120 min etching process under the same conditions. Figure 3 summarizes the initial and final volumes of solution, upon process completion. Regardless of the amount of IPA initially added, given enough time (120 min here) all IPA evaporates and the final solution is only composed of dissolved KOH. The same final volume was achieved with the reference sample (Sample A, without addition of IPA), when applying the same process. From here it can be determined an approximate evaporation rate of 0.0417 mL/min for water vapor, and it can be concluded that the final volume is independent of the IPA content, if sufficient time is given to evaporate all IPA.

Four experiments were conducted to further study IPA influence, as described in Table 1. For example, in Sample 4, from an initial volume of 40 mL (20 mL of KOH dissolved in water and

20 mL of IPA), 27 mL of etchant were available after 60 min. Approximately 2.5 mL of water were evaporated, considering the evaporation rate of 0.0417 mL/min described. Consequently, the remaining difference of 10.5 mL can be attributed to IPA evaporation, thus resulting in an evaporation rate of 0.175 mL/min. The errors in measuring the final volume (some droplets remained inside the HDPE flask) are estimated as a few hundred µL. Table 1 shows the initial KOH and IPA content in solution for each Si wet etch process. The optimal etch time was inferred after periodic microscopic inspections, analyzing whenever the top mesa (Figure 2) would detach from the remaining structure. This corresponds to a full patterned pyramid, with sharp vertices. This optimal etch time is dependent not only of the nominal size of each profile, but also of temperature, KOH concentration and IPA availability. In this work, IPA availability in the solution was tested, thus presenting different optimal etch times, with a time error estimated bellow 5 min, as a consequence of the initial volume of IPA added to the etching solution. At the optimal etch time, the final volume of solution was measured and the dissolved KOH and IPA volumes calculated. Considering initial volumes and evaporation rates, the IPA availability can be calculated (Table 1), representing the amount of time necessary to evaporate all IPA in the etching solution.

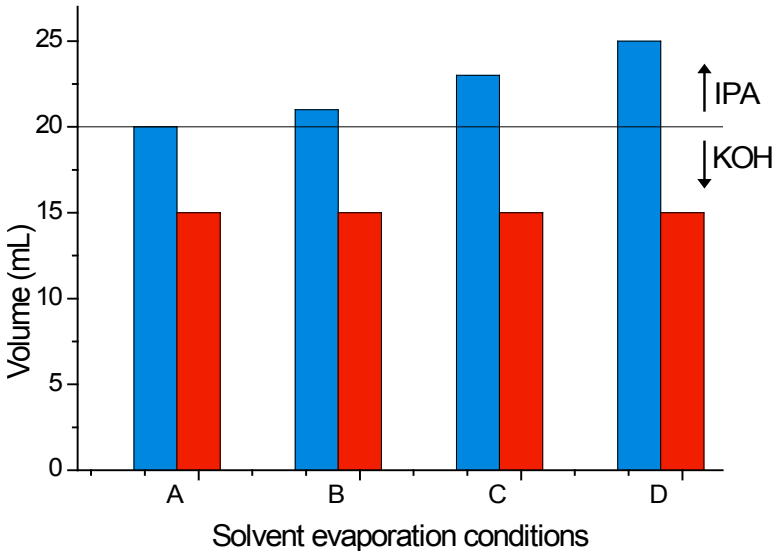

Figure 3. Graphical representation of the total initial volume (blue), as sum of initial KOH volume (20 mL) and IPA volume (0 to 5 mL), *versus* the final volume (red) after a total etching time of 120 min.

Table 1. Experimental conditions used in the definition of 10 µm × 10 µm wide pyramid structures through wet etching. IPA availability represents the predicted time at when all IPA would evaporate. If the "IPA availability" is greater than the "Etch time", the etch process occurs entirely in the presence of IPA. Otherwise, a two phase process would occur (first with dissolved KOH and IPA, followed by dissolved KOH only).

Sample	V_{KOH} (mL)	V_{IPA} (mL)	Etch Time (min)	Final Volume (mL)	IPA Availability (min)
1	20	0	40	18	0
2	20	3	50	18	17
3	20	5	60	17	29
4	20	20	60	27	114

Sample 1 was used as a control sample, where IPA was never added. For Samples 2 and 3, the optimal etch time (50 and 60 min, respectively) was reached after the entire evaporation of IPA from the solution (achieved at 17 and 29 min, respectively). Sample 4 was etched in the presence of IPA during the entire process.

Therefore, IPA influence over the wet etching process of silicon can be measured in terms of availability, rather than concentration. Assuming that IPA is still in the solution, at any given time, and at a macroscopic level, variations in its concentration would not influence its effect. Figure 4 further demonstrates the time evolution of this process.

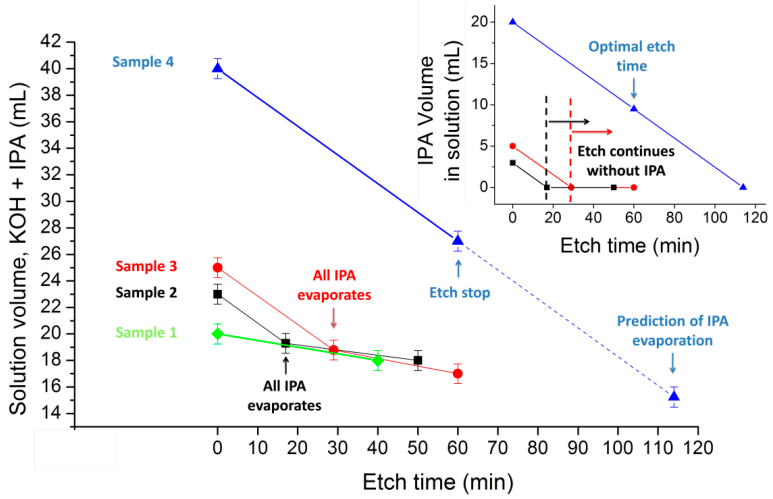

Figure 4. Evolution of solution volumes as a consequence of solvent evaporation. The main chart represents the volume of the whole solution (water and IPA) and the inset chart represents the IPA volume evolution, during the etch process. Sample 1 (green); Sample 2 (black); Sample 3 (red); and Sample 4 (blue).

The IPA availability effect is reinforced by results of a parallel etching process, containing an initial volume of 20 mL dissolved KOH and 2 mL IPA, and then adding 2 mL IPA every 10 min, ensuring that IPA is always available during the entire etching process (evaporation rate of 0.175 mL/min was observed, as previously described). The macroscopic etching results from this experiment are quite similar from those obtained in Sample 4, and distinguishable from every other sample. The same etching profile can be achieved either with an initial saturated solution, or with a lower, but continuously assured, concentration of IPA.

We can support that, after the expected evaporation time has been achieved, the wet etching process will continue in the same conditions as Sample 1 (without IPA). Therefore, we have two specific moments that are particularly relevant to the etching process: when IPA is still present in the solution and when all IPA evaporates.

3.2. Influence of IPA in the Wet Etch of Silicon

The etch rate for the (110) and (331) planes can be 2× and 1.5× larger than the etch rate for the (100) plane, respectively, in KOH etching solutions [12]. This results in a very sharp, but irregular structure with a very marked underetching profile. The obtained structures present an octagon base with a basal diameter up to 1/3 and height up to 1/4 of the profile nominal size (mask size), thus illustrating a severe underetch. However, the etching rate of specific planes in silicon KOH etching can be modulated through IPA. The addition of IPA to the etching solution greatly reduces the etch rate in these planes down to 8× lower [12]. In these conditions, the (110) plane is predominantly protected, thus significantly increasing the base diameter of the structure and reorienting it towards the (100) axis. As the etching undergoes in saturated conditions (where IPA is thoroughly present in the process), the structures maintain a square shape aligned with the axis, whilst increasing base width (Figure 5). Due to this progressive increase and profile spacing, the structures end up colliding upon their edges. Therefore, spacing between adjacent profiles needs to be carefully planned to prevent grouping.

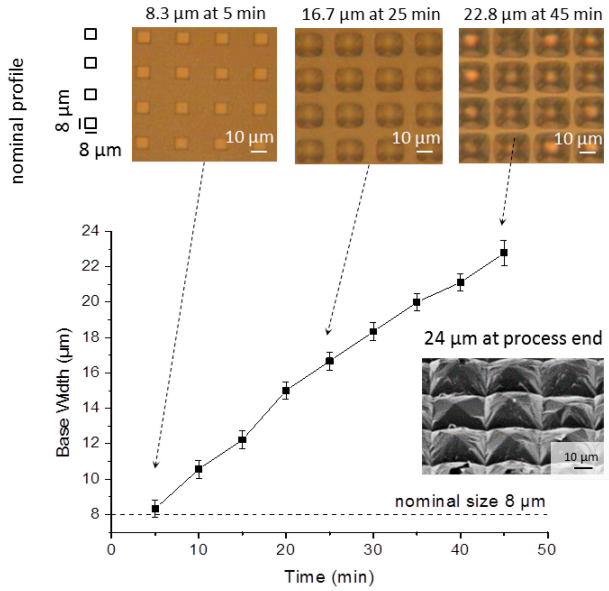

Figure 5. Evolution of base width, along the wet etch process, obtained from a 8 µm × 8 µm square mask with a spacing of 16 µm, under IPA saturated conditions, as described for sample 4 in Table 1. Top view microscope images show how the individual square patterns are enlarged and merged together.

The structure base width starts to recede after complete evaporation of IPA, as a more pronounced (110) etch is performed in the absence of IPA. Moreover, the increase etch rate of the (331) plane promotes the transition from a square shaped to an octagonal shaped structure, as seen in Figure 6. At this stage, this transition occurs progressively, and is independent of the overlaying mask, since the structure width has grown beyond the nominal size, and therefore, is no longer defined by it. As observed in the images representative for the etching process after 80 and 100 min, within Figure 6, the reorientation of the structure shape occurs whilst the initial mask, shown as a bright square, remains overlaid to the dark structure.

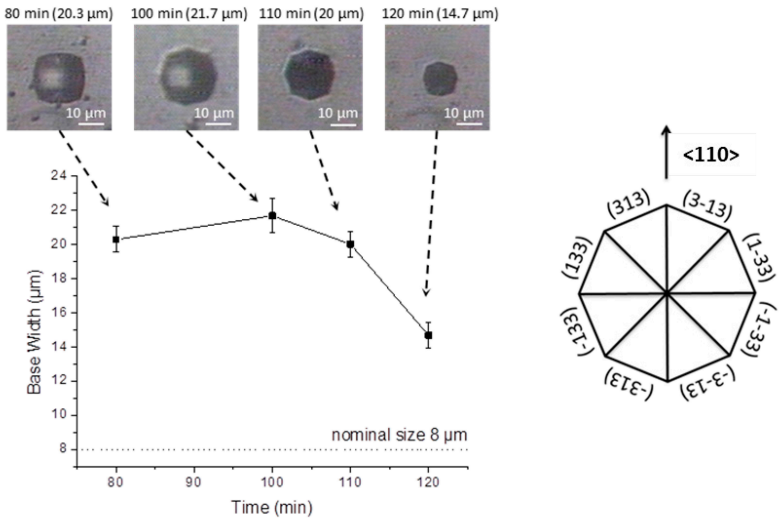

Figure 6. Top view microscopic images demonstrating the evolution of base width, upon the wet etch process, obtained from a 8 µm × 8 µm square mask with a spacing of 40 µm, after IPA evaporation. This process occurred first as described in Figure 5 (up to 80 min), but with an increased spacing as to prevent merging, followed by etching in solution without IPA (after 80 min).

Therefore, modulating the availability of IPA at any given time during the wet etch process allows for a more precise control of the final structure. The initial IPA volume necessary to keep IPA availability until the etch process depends not only on exposed silicon area and the desired etch depth, but also on the volume and surface area of the etching solution.

Each sample was patterned with three mask profiles as depicted in Figure 7: (a) 200 µm wide rectangular mask; (b) 10 µm square mask with a spacing of 20 µm, for v-grove patterning; and (c) 10 µm square mask with a spacing of 20 µm. SEM imaging was used in the determination of pyramid lateral angles. All samples reveal a consistency towards each angles, and by consequence, towards each planes. Three profiles were obtained at same time instants (for each sample, in the same etch solution), and by consequence, with the same IPA availability.

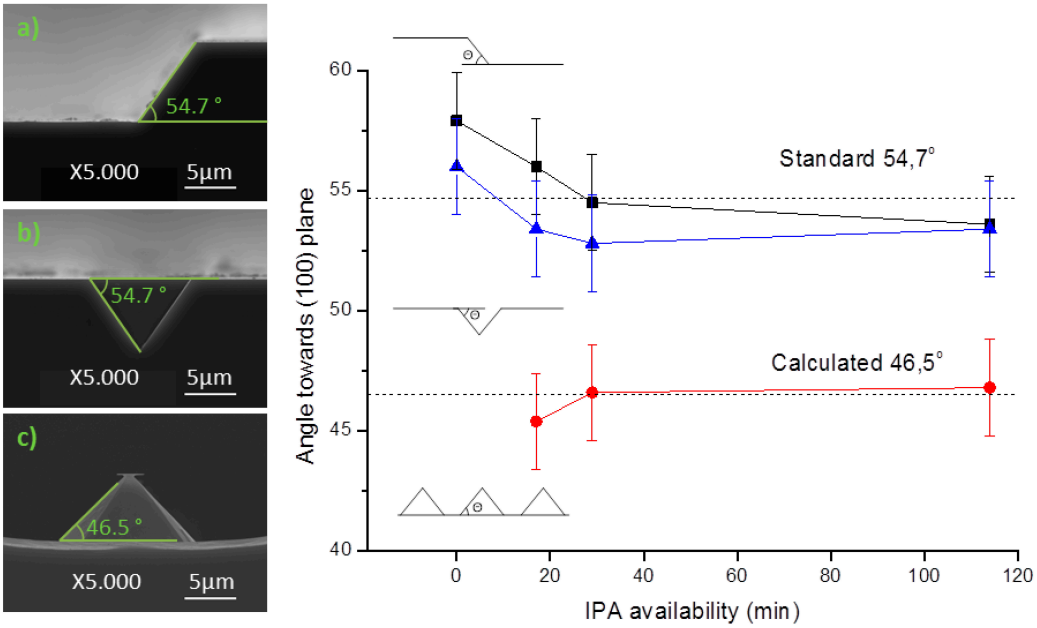

Figure 7. Evolution of measured patterns angle in different IPA availability conditions, obtained from: (**a**) 200 µm wide rectangular mask (black); (**b**) 10 µm v-grove from a square mask with a spacing of 20 µm (blue); and (**c**) 10 µm square mask with a spacing of 20 µm (red).

As seen in Figure 7a,b, the 200 µm wide pattern and the v-groves present a 54.7° ± 2° angle, characteristic of the (111) plane. This result was obtained independently of the IPA volume added to the etch solution, and is in accordance with the expected results. When defining grooves, the etched structure always orientates to align with the wafer flat, forming squared pyramids with (111) planes. IPA influence on the final profile is negligible, either on the base width or profile topography. Typically, the end result is a uniform etch, as in Figure 7b. However, dense structures are deeply influenced by the neighboring topography, which can be seen, in Figure 7c, by the angle decrease to 46.5°. IPA concentration plays little influence in the final patterning result, but its absence originates a structure with a rough etch hardly quantifiable by SEM analysis.

The discrepancy between the results from Figure 7a,c is focused only on the adjacent area around each of the structures. While the first portrays a long line that was patterned 200 µm apart from any other structure, the latter depicts structures patterned in a dense array. The difference can be attributed to microloading effect, in which etchants and byproducts of the reaction have more difficulty diffusing through smaller areas [17]. Therefore, in dense arrays of structures, as soon as the wet etch begins, the (100) plane is less accessible than the (110) plane. In order to modulate this scenario, the desired structures may be patterned further apart, or additives can be incorporated in the etching solution in order to increase the wettability of the silicon wafer. On the contrary, v-groves

are not affected by the microloading effect, and denser arrays of pyramidal structures with sharper edges can be patterned. All the v-grove structures are formed with a square base, independently of the nominal profile shape (mask) or orientation. Figure 8 demonstrates in detail the result of the microloading effect depicted in Figure 7c.

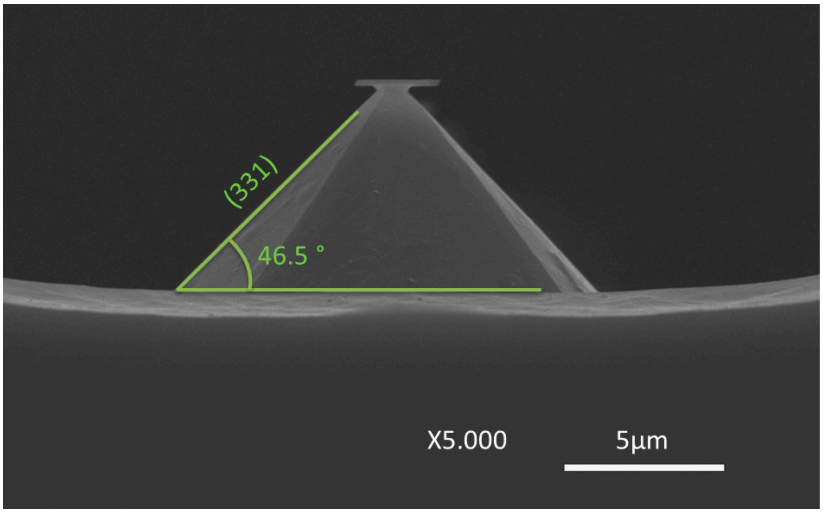

Figure 8. SEM cross-section image of the structure obtained with a 10 µm × 10 µm square mask, spaced 20 µm from the next square, in a 22 wt % KOH wet etch process (Sample 2 in Table 1).

IPA availability takes an important role defining the etched structure in top view SEM images. Near the optimal volume of IPA, the influence on the number of etched planes is maximized. Squares aligned with the wafer flat will have reorientation, initially to a dodecahedron, and finally to an octagon profile, as seen in Figure 9a. This will result in an octagonal pyramid with faces oriented towards the (331) plane.

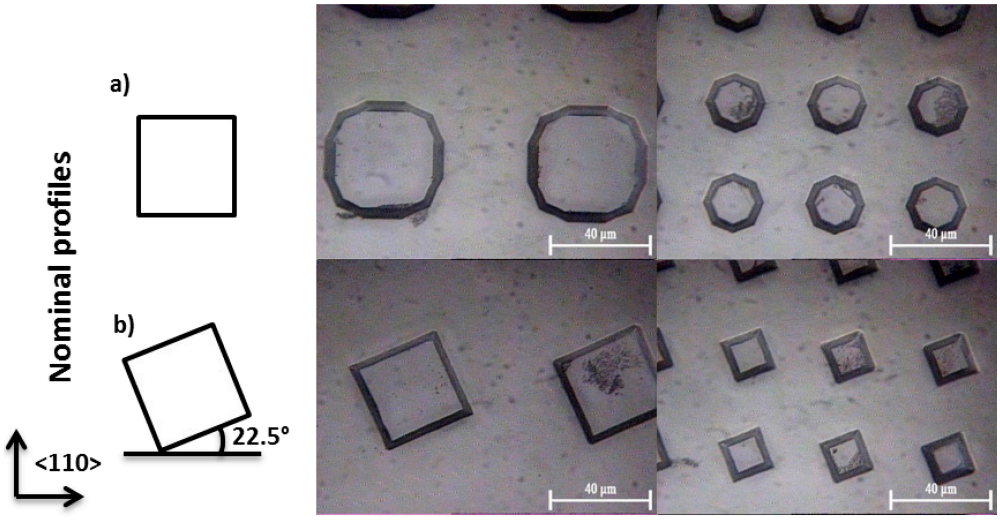

Figure 9. Microscopic inspection of a 22 wt % KOH wet etch process, (Sample 2, in Table 1) after 20 min. Initial profile: (**left**) 40 µm and (**right**) 20 µm; square: (**a**) aligned with the wafer flat; and (**b**) misaligned 22.5° with the wafer flat.

When exposing a squared profile, tilted 22.5°, to the same etching conditions, the result are squared pyramids with no reorientation, as shown in Figure 9b. In fact, this is the same etching

plane that is replicated bi-dimensionally in structures aligned with the wafer flat, such as those in Figure 9a. A predominance to etch in these planes, forming the structural pyramids described in Figure 6, protects those in Figure 9b from any reorientation. An equal result can be obtained when rotating the same misaligned profile by 45°. This way, it is possible to exactly define the desired structure, between a squared and octagonal shape profile, only by modifying the alignment towards the wafer flat.

Alternatively, higher volumes of IPA will form structures with rounder shapes, independently of profile orientation, as demonstrated in Figure 10. The surface topography, however, is much rougher in these conditions and structural uniformity is hard to achieve.

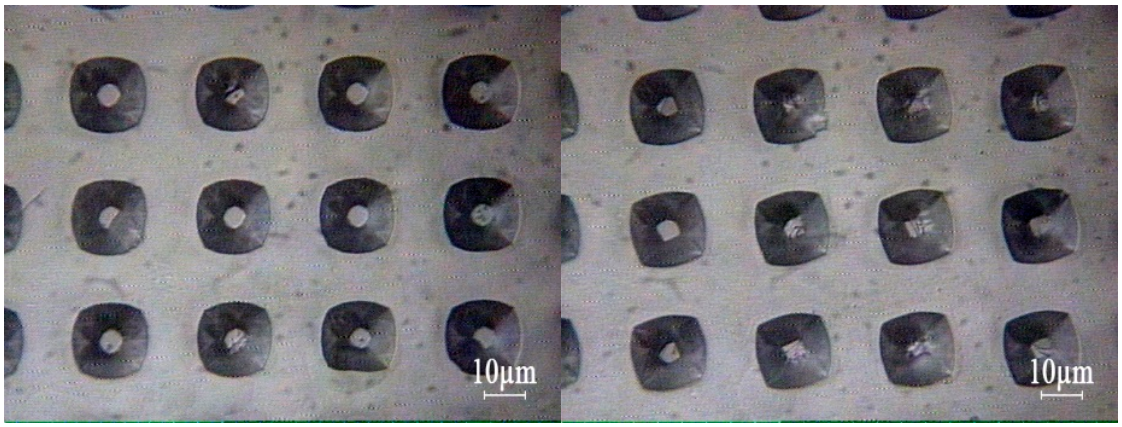

Figure 10. Microscopic inspection of a 22 wt % KOH, saturated with IPA, wet etch process, (Sample 4 in Table 1) after 50 min. Initial profile: 10 µm squares (**left**) aligned and (**right**) misaligned 22.5° with the wafer flat.

An evolution of this process can be observed in Figure 11. As demonstrated previously, in the absence of IPA, the KOH etches the (110) plane predominantly, which causes the visible undercut etch seen in Figure 11a. A 17 min availability of IPA in the beginning of the process is sufficient to stabilize the etching rates for the (110) and (331) planes, thus allowing the formation of octagonal structure (Figure 11b). However, with the increase of IPA availability, the square profile is maintained with rounder edges, as observed in Figure 11c,d.

Figure 11. Microscopic inspection of a 22 wt % KOH wet etch process after 20 min. Initial profile: 40 µm squares aligned with the wafer flat. Conditions are described in Table 1: (**a**) Sample 1; (**b**) Sample 2; (**c**) Sample 3; and (**d**) Sample 4.

Once IPA evaporates, these profiles tend to revert to a situation as in Figure 11a, given the width of the structure is enough to allow for a gradual profile reorientation, before the etching reaches the *mesa* release stage. For the experimental conditions tested, a threshold is held for the IPA availability between 17 and 29 min. However, since the structures observed in Figure 11 are wide enough for the etching to proceed, a longer etching could, eventually, allow for the correction of the etched planes as a consequence of KOH increasing (110) and (331) etch rate.

As a summary, Figure 12 presents a diagram relating the etching profiles obtained along the etching evolution time, with the IPA availability. In general, square patterns are transferred to silicon under a squared-based pyramid (transition from region A to B) whenever a minimum level of IPA is maintained in solution. On the contrary, square based pyramids (region A) may rearrange along etching time into n-side polygons (region C) if meanwhile there is no IPA available in the solution. This transition is gradual and, at any given time, the structure shape is dependent on profile size and etch rate. Continuing the etching until the top mesa is released (optimal etch time) can stabilize the octagonal base pyramidal shape (region D).

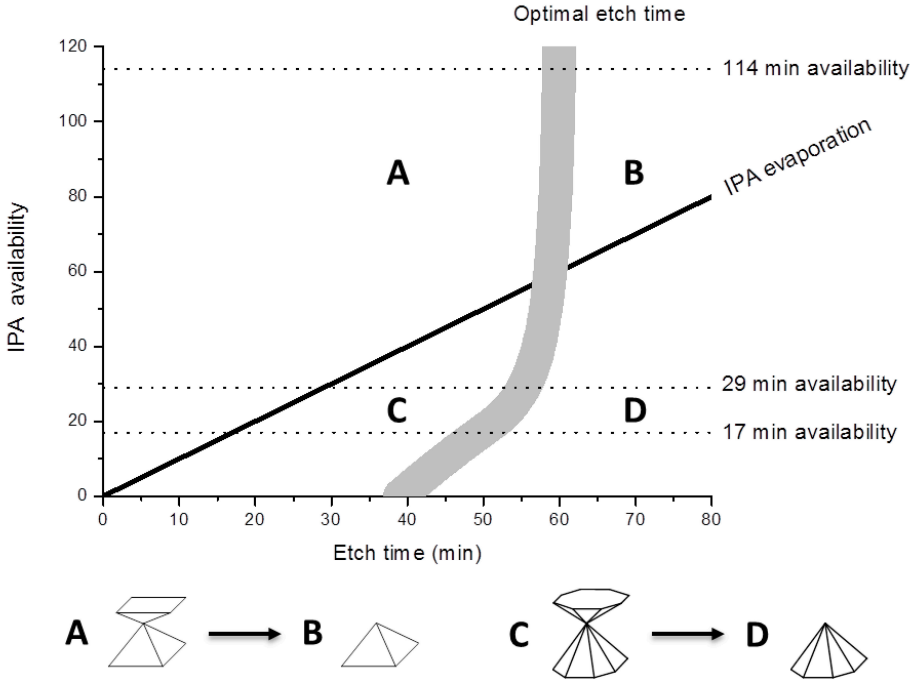

Figure 12. Schematic diagram of the evolution of silicon wet etch structures, under IPA influence, for a 10 μm square mask and the conditions depicted in Table 1.

4. Conclusions

Results demonstrate that IPA availability, and not concentration, plays an important role in the definition of the final structure. When working in an open system, where evaporation affects the chemical balance of the etching solution, we should take into account volumes rather than concentrations. IPA directly reduces the etch rate for the (110) plane, comparatively to the (100) plane. Therefore, longer availability of IPA during a reaction will originate structures with a wider base. However, for a long enough etch, the complete evaporation of IPA will allow the increase etch of the (110) plane, thus receding the base width, and (331) plane, converting square shaped to octagonal shaped structures. Nonetheless, if a steady supply of IPA is constantly added, to assure its availability, the same results are obtained as if a saturated concentration of IPA was always present.

An optimal volume of IPA is desired in order to obtain reproducible structures with the desired size and surface smoothness. In an open system, IPA can be added to the solution at any moment and its availability calculated from the evaporation rate. This fine tailoring of the etching conditions in a dynamic process may open up new possibilities for the precise control of the desired structures.

Acknowledgments: This work was supported by FCT (Fundação para a Ciência e Tecnologia) in the scope of the project PTDC/EBB-EBI/120334/2010 and by FEDER funds through the "Eixo I do Programa Operacional Fatores de Competitividade" (POFC) QREN, project reference COMPETE: FCOMP-01-0124-FEDER-020241. First author thanks FCT for scholarship grant SFRH/BD/74975/2010. INESC-MN and acknowledges Pest-OE/CTM/LA0024/2011 project.

Author Contributions: Tiago Monteiro and Susana Cardoso performed the main work of the dynamic wet etching of silicon. Pamakštys Kastytis helped with the etching angles analysis. Luis Gonçalves, Graça Minas and Susana Cardoso supervised the presented work. All authors have analyzed the results and findings. Tiago Monteiro and Susana Cardoso have written the main manuscript and all authors reviewed the manuscript.

Conflicts of Interest: The authors declare no conflict of interest.

References

1. Gangopadhyay, U.; Kim, K.; Dhungel, S.K.; Basu, P.K.; Yi, J. Low-cost texturization of large-area crystalline silicon solar cells using hydrazine mono-hydrate for industrial use. *Renew. Energy* **2006**, *31*, 1906–1915. [CrossRef]
2. Sparber, W.; Schultz, O.; Biro, D.; Emanuel, G.; Preu, R.; Poddey, A.; Borchert, D. Comparison of texturing methods for monocrystalline silicon solar cells using KOH and Na_2CO_3. In Proceedings of 3rd World Conference on Photovoltaic Energy Conversion, Osaka, Japan, 18 May 2003; pp. 1372–1375.
3. Deng, T.; Chen, J.; Wu, C.N.; Liu, Z.W. Fabrication of inverted-pyramid silicon nanopore arrays with three-step wet etching. *ECS J. Solid State Sci. Technol.* **2013**, *2*, P419–P422. [CrossRef]
4. Xiao, J.; Wang, L.; Li, X.; Pi, X.; Yang, D. Reflectivity of porous-pyramids structured silicon surface. *Appl. Surf. Sci.* **2010**, *257*, 472–475. [CrossRef]
5. Rola, K.; Ptasiński, K.; Zakrzewski, A.; Zubel, I. Silicon 45° micromirrors fabricated by etching in alkaline solutions with organic additives. *Microsyst. Technol.* **2014**, *20*, 221–226. [CrossRef]
6. Indermun, S.; Luttge, R.; Choonara, Y.E.; Kumar, P.; du Toit, L.C.; Modi, G.; Pillay, V. Current advances in the fabrication of microneedles for transdermal delivery. *J. Control. Release* **2014**, *185*, 130–138. [CrossRef] [PubMed]
7. Herwik, S.; Kisban, S.; Aarts, A.A.A.; Seidl, K.; Girardeau, G.; Benchenane, K.; Zugaro, M.B.; Wiener, S.I.; Paul, O.; Neves, H.P.; *et al*. Fabrication technology for silicon-based microprobe arrays used in acute and sub-chronic neural recording. *J. Micromech. Microeng.* **2009**, *19*, 074008. [CrossRef]
8. Seidel, H.; Csepregi, L.; Heuberger, A.; Baumgärtel, H. Anisotropic etching of crystalline silicon in alkaline solutions: I. Orientation dependence and behavior of passivation layers. *J. Electrochem. Soc.* **1990**, *137*, 3612–3626. [CrossRef]
9. Park, S.-H.; Park, J.; You, K.-H.; Shin, H.-C.; Kim, H.-O. Tetramethylammonium hydroxide poisoning during a pallet cleaning demonstration. *J. Occup. Health* **2012**, *55*, 120–124. [CrossRef]
10. Zubel, I.; Kramkowska, M. The effect of isopropyl alcohol on etching rate and roughness of (1 0 0) si surface etched in KOH and TMAH solutions. *Sens. Actuators A Phys.* **2001**, *93*, 138–147. [CrossRef]
11. Drago, R.; Vrtacnik, D.; Aljancic, U.; Amon, S. Effective roughness reduction of {100} and {311} planes in anisotropic etching of {100} silicon in 5% TMAH. *J. Micromech. Microeng.* **2003**, *13*, 26.
12. Zubel, I.; Kramkowska, M. Etch rates and morphology of silicon (h k l) surfaces etched in KOH and KOH saturated with isopropanol solutions. *Sens. Actuators A Phys.* **2004**, *115*, 549–556. [CrossRef]
13. Rola, K.; Zubel, I. Impact of alcohol additives concentration on etch rate and surface morphology of (100) and (110) si substrates etched in koh solutions. *Microsyst. Technol.* **2013**, *19*, 635–643. [CrossRef]
14. Palik, E.D.; Gray, H.F.; Klein, P.B. A raman study of etching silicon in aqueous KOH. *J. Electrochem. Soc.* **1983**, *130*, 956–959. [CrossRef]
15. Yang, C.-R.; Chen, P.-Y.; Chiou, Y.-C.; Lee, R.-T. Effects of mechanical agitation and surfactant additive on silicon anisotropic etching in alkaline KOH solution. *Sens. Actuators A Phys.* **2005**, *119*, 263–270. [CrossRef]
16. INESC-MN. Available online: http://www.inesc-mn.pt (accessed on 9 October 2015).
17. Waser, R.; Keller, H.; Erb, U. *Nanoelectronics and Information Technology: Advanced Electronic Materials and Novel Devices*; John Wiley & Sons, Inc.: Hoboken, NJ, USA, 2003; p. 1002.